Title

The α-Arrestin ARRDC3 Regulates the Endosomal Residence Time and Intracellular Signaling of the β2-Adrenergic Receptor*

Journal

Journal of Biological Chemistry, 291(28)

ISSN

0021-9258

Authors

Tian, Xufan
Irannejad, Roshanak
Bowman, Shanna L
et al.

Publication Date

2016-07-01

DOI

10.1074/jbc.m116.716589

Peer reviewed

THE JOURNAL OF BIOLOGICAL CHEMISTRY VOL. 291, NO. 28, pp. 14510–14525, July 8, 2016

The α-Arrestin ARRDC3 Regulates the Endosomal Residence Time and Intracellular Signaling of the β_2-Adrenergic Receptor*

Received for publication, January 19, 2016, and in revised form, May 11, 2016 Published, JBC Papers in Press, May 11, 2016, DOI 10.1074/jbc.M116.716589

Xufan Tian[‡], Roshanak Irannejad[§], Shanna L. Bowman[¶], Yang Du[‖], Manojkumar A. Puthenveedu[¶], Mark von Zastrow[§], and Jeffrey L. Benovic[‡1]

From the [‡]Department of Biochemistry and Molecular Biology, Thomas Jefferson University, Philadelphia, Pennsylvania 19107, the [§]Department of Psychiatry, University of California at San Francisco, San Francisco, California 94158, the [¶]Department of Biological Sciences, Carnegie Mellon University, Pittsburgh, Pennsylvania 15213, and the [‖]Department of Molecular and Cellular Physiology, Stanford University School of Medicine, Stanford, California 94305

Arrestin domain-containing protein 3 (ARRDC3) is a member of the mammalian α-arrestin family, which is predicted to share similar tertiary structure with visual-/β-arrestins and also contains C-terminal PP*X*Y motifs that mediate interaction with E3 ubiquitin ligases. Recently, ARRDC3 has been proposed to play a role in regulating the trafficking of G protein-coupled receptors, although mechanistic insight into this process is lacking. Here, we focused on characterizing the role of ARRDC3 in regulating the trafficking of the β_2-adrenergic receptor (β_2AR). We find that ARRDC3 primarily localizes to EEA1-positive early endosomes and directly interacts with the β_2AR in a ligand-independent manner. Although ARRDC3 has no effect on β_2AR endocytosis or degradation, it negatively regulates β_2AR entry into SNX27-occupied endosomal tubules. This results in delayed recycling of the receptor and a concomitant increase in β_2AR-dependent endosomal signaling. Thus, ARRDC3 functions as a switch to modulate the endosomal residence time and subsequent intracellular signaling of the β_2AR.

G protein-coupled receptor (GPCR)[2] signaling is, in part, tightly regulated by the availability of the receptors on the cell surface (1). In general, upon agonist stimulation, GPCRs initiate signaling by coupling to heterotrimeric G proteins at the plasma membrane (2). Prolonged agonist stimulation often leads to receptor phosphorylation by GPCR kinases, β-arrestin recruitment, and receptor internalization via β-arrestin-mediated interaction with clathrin-coated pits (3, 4). Once a GPCR is internalized, it either recycles back to the plasma membrane or is sorted for degradation via the endosome-lysosome pathway (5).

It was traditionally thought that acute G protein-mediated signaling terminated once the receptor was phosphorylated and bound β-arrestin and that the receptor could only fully resume its ability to activate G protein signaling once it was internalized, dephosphorylated, and recycled back to the plasma membrane (1). However, it has been recently appreciated that activated GPCRs, such as the β_2-adrenergic receptor (β_2AR) (6) and thyroid-stimulating hormone receptor (7, 8), can also mediate acute G protein-dependent signaling on endosomes (9).

Recently, α-arrestins, a subgroup of the arrestin clan that also includes visual-/β-arrestins and VPS26-related proteins, have been suggested to regulate cell surface transporter and GPCR endocytic trafficking (5). For example, yeast α-arrestins serve as adaptor proteins for E3 ubiquitin ligases and regulate cell surface transporter degradation in response to stress (10, 11). In mammals, there are six α-arrestins, named arrestin-domain containing protein (ARRDC) 1–5 and thioredoxin-interacting protein. Sequence comparison suggests the following two fundamental differences between mammalian α-arrestins and visual-/β-arrestins that could potentially functionally differentiate these two subclans in cells: 1) α-arrestins appear to lack a "polar core" (12) that functions in maintaining visual-/β-arrestins in their "basal conformation" and is crucial for their phosphosensing activity (13); and 2) most α-arrestins contain PP*X*Y motifs in their C-tails that visual-/β-arrestins lack (11, 12, 14). PP*X*Y motifs often interact with WW-domains, and ARRDCs have been shown to interact with the WW-domain of various HECT-domain E3 ubiquitin ligases (15–17). Indeed, the first PP*X*Y motif of ARRDC3 has been shown to interact with the third WW domain of Nedd4 with high affinity *in vitro* (18). Mutations of either the PP*X*Y motifs of ARRDC3 or WW domains of Nedd4 inhibit the interaction between these two proteins in cells (15, 18).

Recently, a role for ARRDC3 in β_2AR endocytic trafficking has been proposed. Nabhan *et al.* (15) reported that ARRDC3 primarily acts at the plasma membrane where it interacts with the β_2AR in an agonist-dependent manner and functions to facilitate Nedd4-mediated ubiquitination and subsequent degradation of the β_2AR. In contrast, Han *et al.* (19) showed that overexpression or depletion of ARRDC3 does not affect β_2AR ubiquitination, internalization, or degradation. In fact, their

* This work was supported by National Institutes of Health Grants R37 GM047417 and R01 GM068857 (to J. L. B.), R01 DA010711 (to M. v. Z.), R21 DA036086 (to M. A. P.), K99 HL122508 (to R. I.), and T32 NS007433 (to S. L. B.). The authors declare that they have no conflicts of interest with the contents of this article. The content is solely the responsibility of the authors and does not necessarily represent the official views of the National Institutes of Health.

[1] To whom correspondence should be addressed. Tel.: 215-503-4607; Fax: 215-503-5393; E-mail: jeffrey.benovic@jefferson.edu.

[2] The abbreviations used are: GPCR, G protein-coupled receptor; β_2AR, β_2-adrenergic receptor; TfR, transferrin receptor; BRET, bioluminescence resonance energy transfer; ISO, isoproterenol; ARRDC, arrestin domain-containing protein.

study suggested that the ARRDC3 siRNA used by Nabhan *et al.* (15) could also knockdown β-arrestin expression and that it was β-arrestin that mediated β_2AR ubiquitination and degradation, and not ARRDC3. They also demonstrated that endosomal localized ARRDC3 co-localized with internalized β_2AR. Although these findings are intriguing, it is evident that the role of ARRDCs in β_2AR trafficking, if any, has not been clearly defined.

In this study, we investigated the role of ARRDC3 in β_2AR trafficking by evaluating the following: 1) the cellular localization of ARRDC3; 2) ARRDC3 interaction with the β_2AR; and 3) the role of ARRDC3 in β_2AR endocytic trafficking and endosomal signaling. We find that ARRDC3 is mainly localized to EEA1-positive early endosomes, where it interacts with the ESCRT-0 complex. ARRDC3 associates with the β_2AR in a ligand-independent manner and regulates β_2AR recycling by negatively regulating β_2AR entry into recycling tubules, thereby retaining it on EEA1-positive early endosomes. Consequently, ARRDC3 modulates receptor-dependent G protein signaling on endosomes.

Results

ARRDC3 Is Localized on EEA1-positive Early Endosomes and Interacts with the ESCRT-0 Complex—To evaluate the cellular localization of ARRDC3, we initially transfected GFP-tagged wild type ARRDC3 or a GFP-tagged PP*X*Y mutant ARRDC3 (ARRDC3-AASA/AALA) in HEK293 cells. Using fixed cell immunofluorescence microscopy, we found that ARRDC3 is mainly localized to endocytic vesicles, although ARRDC3-AASA/AALA is primarily at the plasma membrane (Fig. 1*A*). Using EEA1, LAMP1, and giantin antibody staining as early endosome, late endosome/lysosome, and trans-Golgi network markers, respectively, we found that ARRDC3 mainly co-localized with EEA1 on EEA1-positive early endosomes (Fig. 1*B*). To assess the localization of endogenous ARRDC3, we co-immunostained ARRDC3 and EEA1/LAMP1 in BT549 cells, a breast cancer cell line that has a 5–10-fold higher expression level of endogenous ARRDC3 compared with HEK293 cells (Fig. 1, *C* and *D*). Importantly, endogenous ARRDC3 co-localized with EEA1 in BT549 cells, although the staining was lost by treatment with an ARRDC3-specific siRNAs that effectively knocked down expression (Fig. 1*D*). There was no apparent co-localization of ARRDC3 with LAMP1 in these cells. Thus, ARRDC3 is primarily localized on EEA1-positive early endosomes.

To further evaluate the endosomal localization of ARRDC3, we co-expressed FLAG-tagged STAM-1, a component of the ESCRT-0 complex that primarily localizes to early endosomes (20), and HA-tagged ARRDC3 in HEK293 cells. Immunoprecipitation studies showed that ARRDC3 co-immunoprecipitates with STAM-1 (Fig. 2*A*). In contrast, ARRDC3-AASA/AALA, which is primarily localized at the plasma membrane, did not co-immunoprecipitate with STAM-1 (Fig. 2*A*). Because the ESCRT-0 complex has been reported to localize to discrete microdomains of EEA1-positive early endosomes (21), we hypothesized that ARRDC3 would localize to the same microdomains as STAM-1. To better visualize early endosomes, we transiently transfected HEK293 cells with Rab5Q79L, a Rab5 mutant that enhances homotypic early endosome fusion and results in enlarged early endosomes (22). Immunofluorescence microscopy and associated line scan analysis demonstrated that ARRDC3 and endogenous STAM co-localized to the same early endosome microdomains (Fig. 2*B*). Taken together, we conclude that ARRDC3 interacts with the ESCRT-0 complex on EEA1-positive early endosomes.

One PPXY Motif Is Needed to Localize ARRDC3 to Endosomes—Because ARRDC3-AASA/AALA was primarily localized at the plasma membrane, we next determined whether both PP*X*Y motifs are required to localize ARRDC3 to endosomes. Both GFP-tagged ARRDC3-AASA and ARRDC3-AALA showed strong endosomal localization similar to wild type ARRDC3 (Fig. 2*C*), suggesting that one PP*X*Y motif is sufficient to mediate ARRDC3 localization to early endosomes. We also tested whether the C-tail of ARRDC3, which contains both PP*X*Y motifs, is sufficient for endosomal localization. The GFP-tagged ARRDC3 C-tail was primarily cytoplasmic with a localization pattern similar to GFP alone (Fig. 2*C*). This suggests that the arrestin-like domain of ARRDC3 is also important for the endosomal localization of ARRDC3.

Because ARRDC3 interacts with Nedd4 family ubiquitin ligases via its PP*X*Y motifs (15, 18, 19), we tested whether ARRDC3 was ubiquitinated and, if so, whether the ubiquitination status of ARRDC3 played a role in its localization. We monitored the ubiquitination status of transfected GFP-tagged wild type and mutant ARRDC3 by immunoprecipitating ARRDC3 and blotting for endogenous ubiquitin. Although ARRDC3 was clearly ubiquitinated, ARRDC3-AASA/AALA appeared to undergo no ubiquitination. Moreover, both ARRDC3-AASA and ARRDC3-AALA were also ubiquitinated, although ARRDC3-AASA appeared to undergo less ubiquitination (Fig. 2*D*). These observations demonstrate that only one of the PP*X*Y motifs is needed to facilitate ARRDC3 ubiquitination. Taken together, we conclude that at least one PP*X*Y motif as well as the arrestin-like domain are required to mediate ARRDC3 localization to endosomes. Although the endosomal localization of ARRDC3 is positively correlated with its ubiquitination state, we do not know whether ubiquitination is required for endosomal localization.

ARRDC3 Interacts with the β_2AR in a Ligand-independent Manner—To evaluate whether ARRDC3 interacts with the β_2AR, we transiently co-transfected FLAG-tagged β_2AR with either HA-tagged ARRDC3 or HA-tagged β-arrestin2 in HEK293 cells. The cells were treated with or without agonist and lysed, and then FLAG-β_2AR was immunoprecipitated and analyzed for co-immunoprecipitation of ARRDC3 or β-arrestin2. As expected, β-arrestin2 co-immunoprecipitation with the β_2AR was markedly increased by agonist treatment (Fig. 3*A*). ARRDC3 also co-immunoprecipitated with the β_2AR, although the degree of interaction was not affected by isoproterenol (ISO) (Fig. 3*A*). These observations were confirmed using a bioluminescence resonance energy transfer (BRET) assay, which monitors protein-protein interaction in living cells (23). Upon ISO stimulation, the BRET ratio of β_2AR-RlucII and GFP10-β-arrestin2 rapidly increased over the 30-min time course (Fig. 3*B*). In contrast, the BRET ratio of β_2AR-RlucII and GFP10-ARRDC3 was high at time 0 and was largely unaffected by the addition of isoproterenol (Fig. 3*B*). This suggests that the

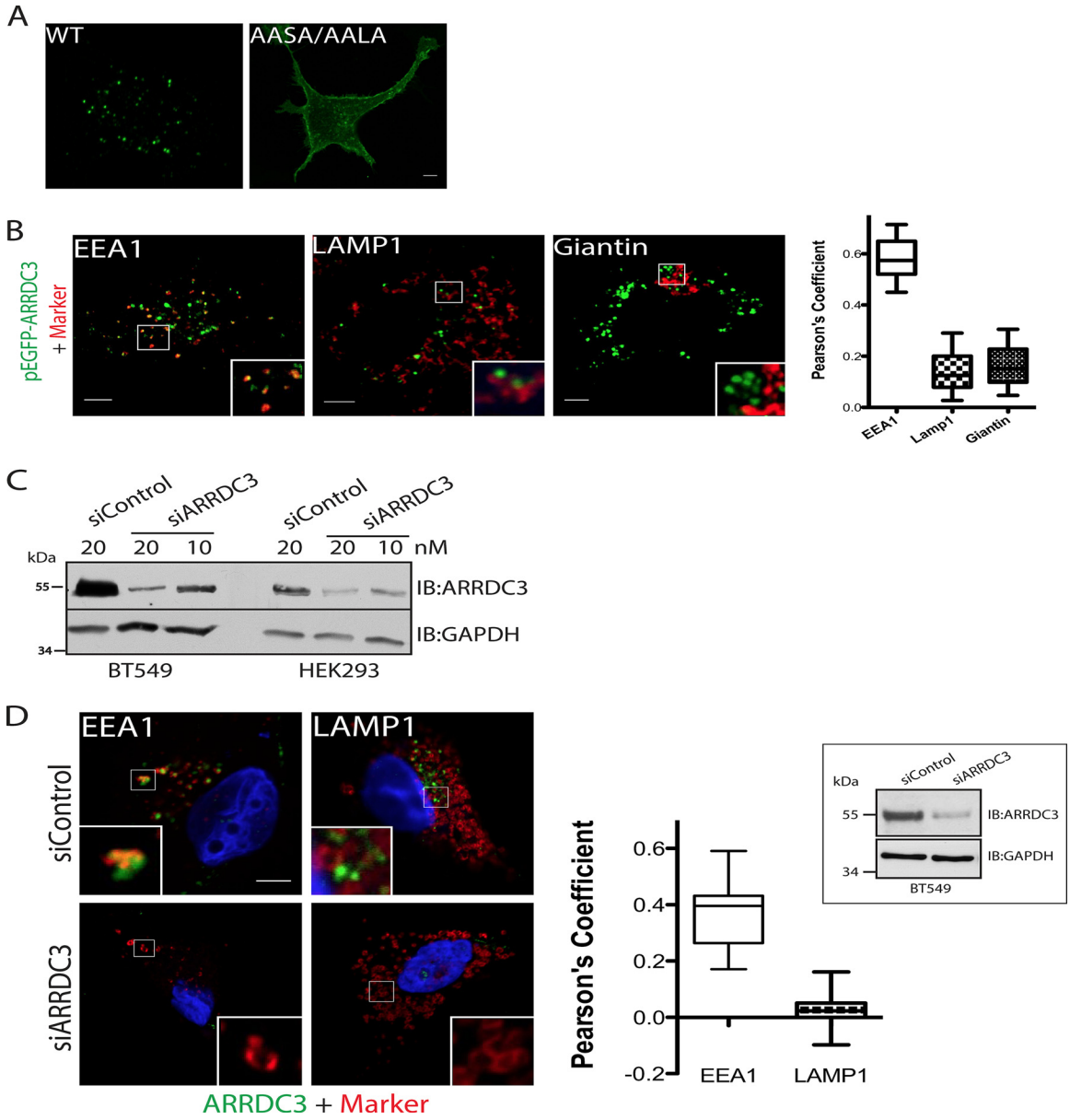

FIGURE 1. **ARRDC3 is primarily localized to EEA1-positive early endosomes.** *A,* representative immunofluorescence images show the localization of transiently transfected pEGFP-ARRDC3 and pEGFP-AASA/AALA in HEK293 cells (from $n > 5$). *B,* representative immunofluorescence images and co-localization analyses of transiently transfected pEGFP-ARRDC3 (shown in *green*) with endocytic markers (shown in *red*) in HEK293 cells. $n = 25$. Data points are represented as mean, min to max. *C,* Western blot analysis evaluating the expression level of endogenous ARRDC3 and effectiveness of siRNA knockdown in HEK293 and BT549 cells. 50 μg of whole cell lysate was loaded in each lane. *D,* representative immunofluorescence images and co-localization analyses demonstrating the co-localization of endogenous ARRDC3 (shown in *green*) and EEA1/LAMP1 (shown in *red*) in BT549 cells. Western blotting is used to evaluate the degree of endogenous ARRDC3 depletion by siRNA. $n = 25$. Data points are represented as mean, min to max. *Scale bars,* 5 μm. *IB,* immunoblot.

β_2AR and ARRDC3 interact in an agonist-independent manner. We also treated cells expressing the β_2AR-RlucII and GFP10-ARRDC3 with the β_2AR inverse agonists, propranolol and ICI 118,551, and again found no effect on the BRET ratio (Fig. 3*C*). To verify that this was a true measure of β_2AR-ARRDC3 interaction, we performed a bystander BRET analysis by varying the ratio of GFP10-ARRDC3 to β_2AR-RlucII. Indeed, the BRET ratio increased hyperbolically as a function of increasing GFP10/RlucII ratio, and saturation was reached indicating that all β_2AR-RlucII was associated with GFP10-ARRDC3 (Fig. 3*D*). These results support the conclusion that the high BRET ratio between the β_2AR-RlucII and GFP10-ARRDC3 is indeed a result of protein-protein interaction. To further support these results, we performed an *in vitro* pull-down assay using purified FLAG-tagged β_2AR in the presence or absence of ISO or propranolol along with *in vitro* translated ^{35}S-labeled ARRDC3. ARRDC3 was able to bind to the β_2AR, and this binding was unaffected by ligand (Fig. 3*E*). Taken together, our data demonstrate that ARRDC3 directly interacts with the β_2AR in a ligand-independent manner.

It was noticeable that a higher BRET ratio was observed at time 0 in β_2AR-RlucII and GFP10-ARRDC3 co-transfected cells (Fig. 2*B*), suggesting some association between these proteins under steady state. Because the β_2AR is primarily localized to the plasma membrane while ARRDC3 is at the endosome in unstimulated cells (Fig. 1*A*), it was puzzling how

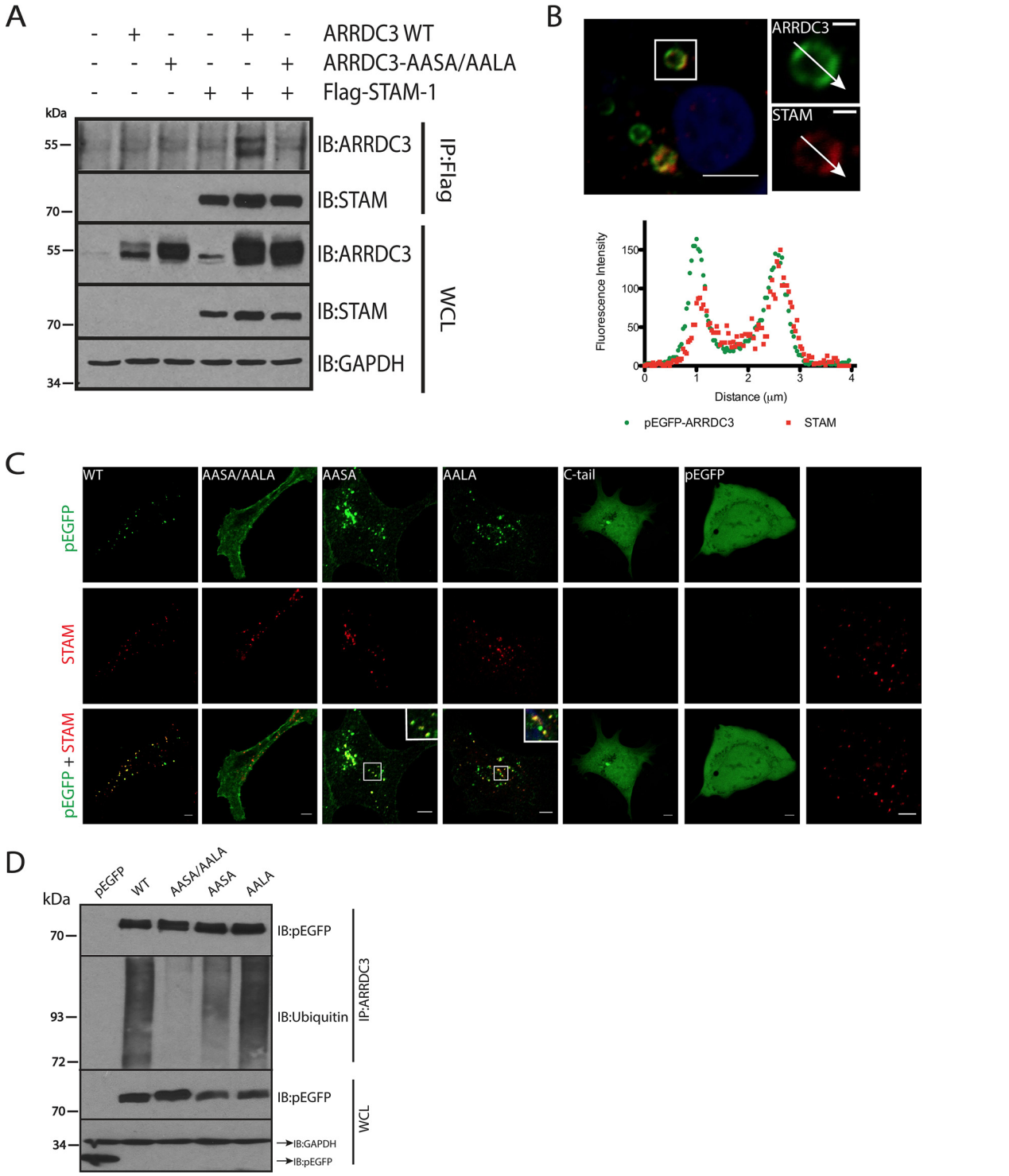

FIGURE 2. **ARRDC3 is ubiquitinated and interacts with the ESCRT-0 complex.** *A,* co-immunoprecipitation of transiently transfected pEGFP-ARRDC3 or pEGFP-ARRDC3-AASA/AALA with FLAG-STAM-1 in HEK293 cells. *B,* representative immunofluorescence images and corresponding line scan analysis demonstrating the co-localization of expressed pEGFP-ARRDC3 and endogenous STAM on endosomes in HEK293 cells. Endosomes were enlarged by transient transfection of Rab5-Q79L. *Scale bars* of the *insets*, 1 μm. *C, top,* representative immunofluorescence images are shown to demonstrate the localization of WT and mutant pEGFP-ARRDC3 in HEK293 cells. *Middle* and *bottom*, same cells were co-stained for endogenous STAM to evaluate the co-localization with the ESCRT-0 complex. *D,* ubiquitination of WT and mutant GFP-ARRDC3 was evaluated by immunoprecipitating ARRDC3 followed by detection of endogenous ubiquitin by Western blotting. All experiments are done at least three times. *Scale bars,* 5 μm. *WCL*, whole cell lysate; *IB*, immunoblot.

ARRDC3 and β_2AR would exhibit a significant BRET ratio before receptor activation. To address this question, we transiently transfected pEGFP-ARRDC3 in HEK293 cells stably expressing FLAG-tagged β_2AR (24). The cells were fixed, permeabilized, and then immunostained with FLAG antibody to visualize the β_2AR. Surprisingly, in GFP-ARRDC3-expressing cells, a noticeable endosomal co-localization of β_2AR and ARRDC3 was observed in unstimulated cells (Fig. 3*F*). This

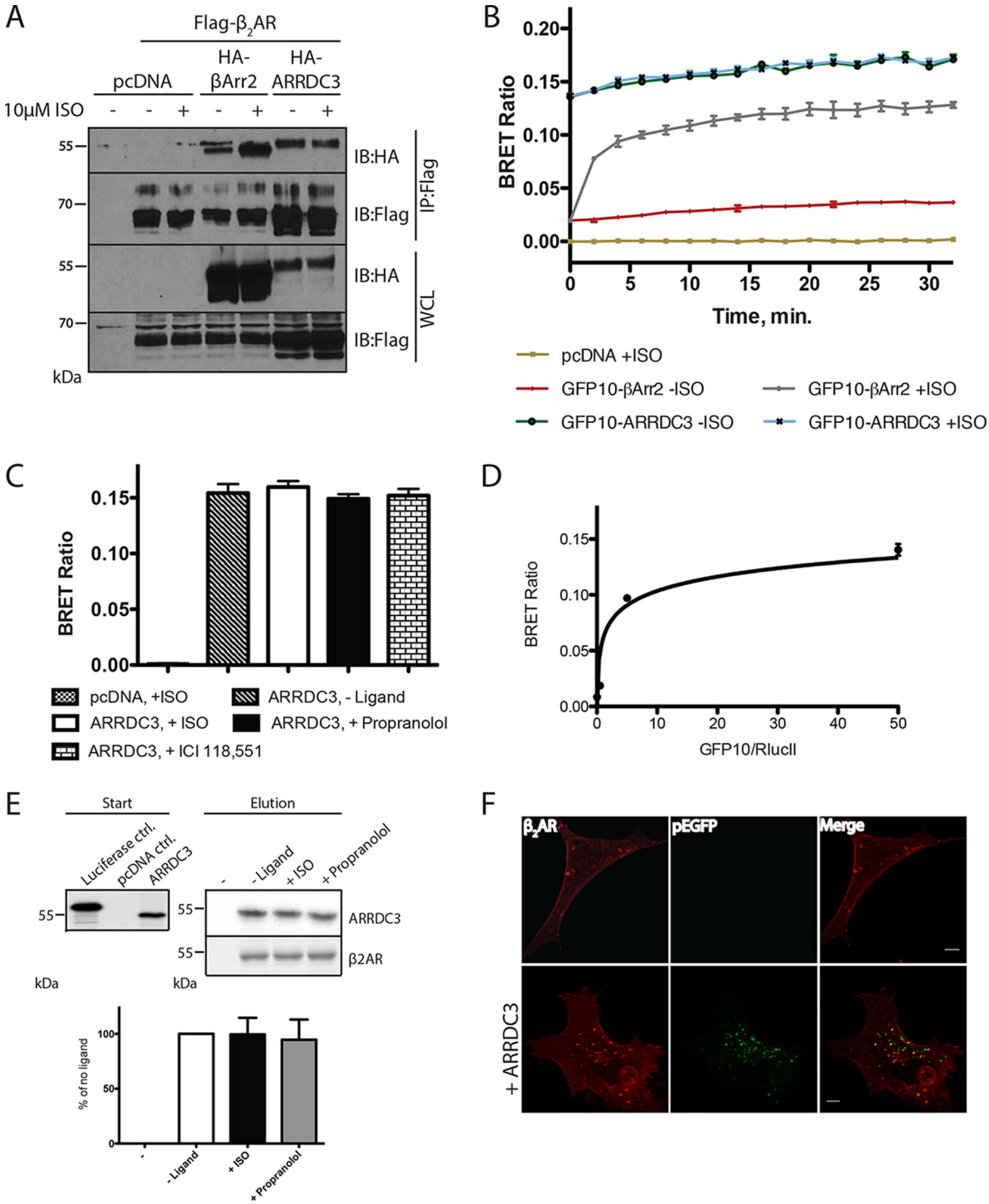

FIGURE 3. **ARRDC3 directly interacts with the β_2AR in a ligand-independent manner.** Co-immunoprecipitation (A) and BRET analysis (*B*) were performed to assess the interaction of the β_2AR and ARRDC3 using β-arrestin2 as a control. The increased β_2AR expression level in ARRDC3 co-expressed samples shown in *A, 6th* and *7th lanes,* is not reproducible. Cells were treated ±10 μM ISO for 25 min. Experiments were done at least three times. Representative data are shown. *C,* BRET analysis was performed to evaluate the interaction of the β_2AR and ARRDC3 upon treating cells with indicated ligands. BRET ratio was taken at 15 min. $n = 3$. Representative data are shown. Data are represented as mean ± S.D. *D,* bystander BRET analysis with increased amounts of GFP10-ARRDC3 to a fixed concentration of β_2AR-RlucII. $n = 3$. Representative data are shown. Data are represented as mean ± S.D. *E, in vitro* pulldown assay was performed to assess the interaction of the purified β_2AR and *in vitro* translated ^{35}S-labeled ARRDC3. The β_2AR was either unliganded or bound with ISO or propranolol. $n = 5$. Representative data are shown. Data are represented as mean ± S.E. *F,* representative fixed cell immunofluorescence images show the localization of the β_2AR in FLAG-β_2AR-stable HEK293 cells transiently transfected with vector or pEGFP-ARRDC3. *Scale bars,* 5 μm. *WCL,* whole cell lysate; *IB,* immunoblot.

likely explains the basal level of β_2AR and ARRDC3 interaction suggested by the high BRET ratio at time 0.

ARRDC3 Regulates β_2AR Recycling—We next examined the functional role of ARRDC3 in β_2AR endocytic trafficking. We hypothesized that ARRDC3 would not affect β_2AR internalization due to the endosomal localization of ARRDC3 (Fig. 1, *A* and *B*). We transiently transfected either vector control or ARRDC3 in a HEK293 cell line stably expressing FLAG-β_2AR

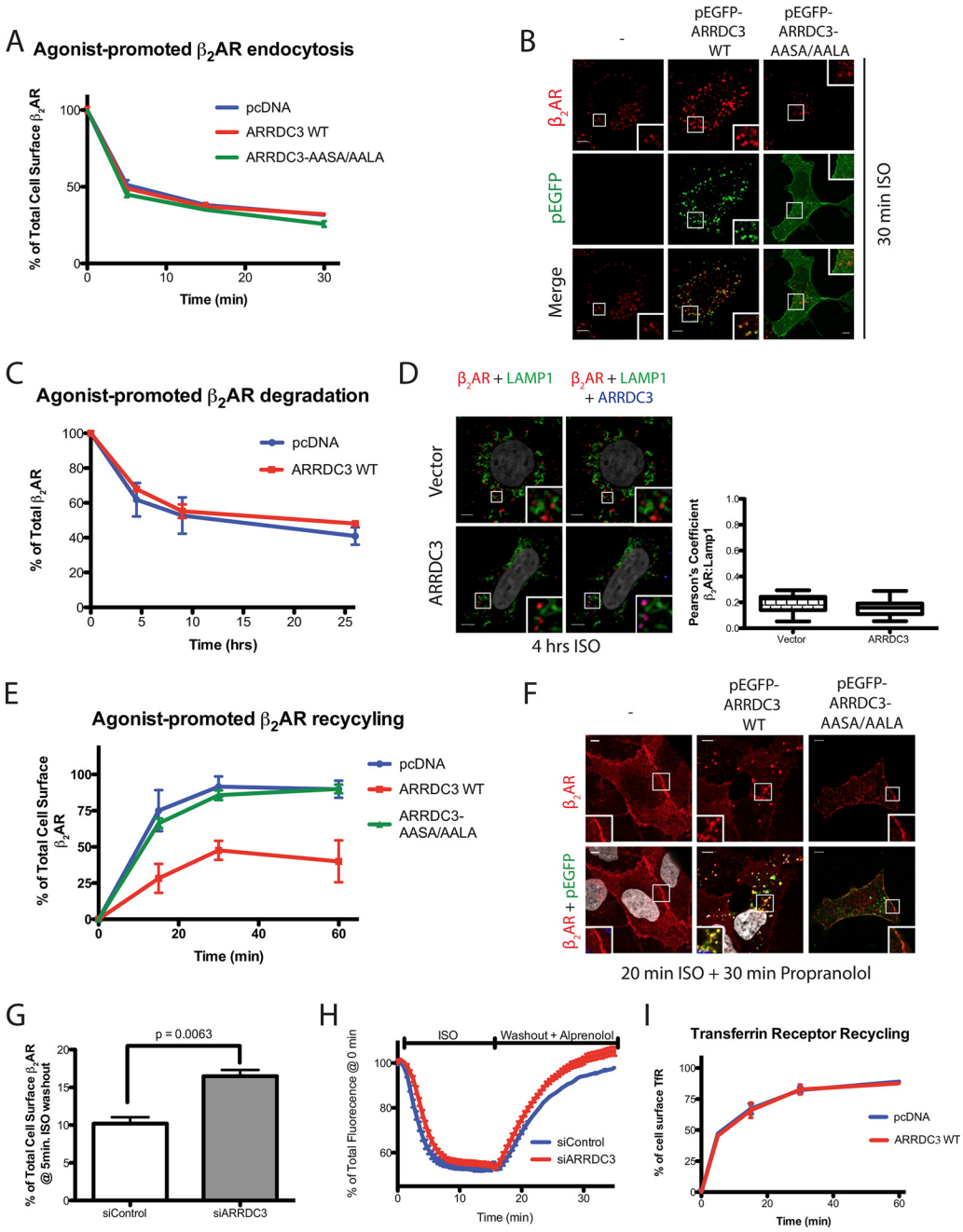

FIGURE 4. **ARRDC3 regulates agonist-induced β_2AR recycling.** *A,* rate of β_2AR internalization was evaluated by cell surface ELISA. Cells were transiently transfected with vector, ARRDC3, or ARRDC3-AASA/AALA in FLAG-β_2AR-stable HEK293 cells. $n = 3$. Data are represented as mean ± S.D. *B,* immunofluorescence staining and co-localization of the β_2AR and ARRDC3 or ARRDC3-AASA/AALA upon 20 min of treatment with 10 μM ISO in FLAG-β_2AR-stable HEK293 cells. *C,* total amount of β_2AR present in β_2AR-stable HEK293 cells at each ISO-treated time point was assessed by [^{125}I]iodocyanopindolol binding assay. The *graph* represents the mean ± S.D. from three independent experiments. *D,* immunofluorescence staining and co-localization analysis, demonstrated by Pearson's coefficient, of the β_2AR, ARRDC3, and the lysosomal marker LAMP1, upon a 4-h treatment with 10 μM ISO in β_2AR-stable HEK293 cells. Representative images are shown. Pearson's coefficient is the mean ± S.D. from $n = 30$. *E,* flow cytometric analysis of the β_2AR recycling by uptake and efflux of cell surface-labeled M1 anti-FLAG antibody in FLAG-β_2AR-stable HEK293 cells transiently transfected with vector, ARRDC3, or ARRDC3-AASA/AALA. The *graph* represents the mean ± S.D. from three independent experiments. *F,* representative immunofluorescence staining and co-localization of the β_2AR and ARRDC3 or ARRDC3-AASA/AALA upon 20 min of treatment with 10 μM ISO followed by a 30-min incubation with 10 μM propranolol. *G,* flow cytometric analysis of β_2AR recycling by uptake and efflux of cell surface-labeled M1 anti-FLAG antibody in FLAG-β_2AR-stable HEK293 cells transfected with siControl or siARRDC3. The *graph* represents the mean ± S.D. from three independent experiments. Unpaired *t* test. *H,* quantitation of fluorescence changes of SpH-β_2AR demonstrating a rapid loss of surface β_2AR level in response to 10 μM ISO treatment and recovery in response to washout with 10 μM alprenolol in SpH-β_2AR-stable HEK293 cells transfected with siControl or siARRDC3. Fluorescence values were normalized to initial values from multiple cells (n >1,500 cells analyzed). *I,* flow cytometric analysis of TfR recycling by uptake and efflux of cell surface-labeled transferrin. The *graph* represents the mean ± S.D. from three independent experiments. *Scale bars,* 5 μm.

and monitored the rate of agonist-promoted β_2AR internalization using a cell surface ELISA (25). A similar rate of β_2AR internalization was observed in cells transfected with either vector control, wild type ARRDC3, or ARRDC3-AASA/AALA (Fig. 4*A*). These findings were also supported by fixed cell immunostaining, which showed that cell surface β_2ARs were

comparably localized to endocytic vesicles in vector control, ARRDC3, and ARRDC3-AASA/AALA transfected cells following 20 min of ISO treatment (Fig. 4*B*). Furthermore, knocking down endogenous ARRDC3 using an ARRDC3-specific siRNA also had no effect on the extent of agonist-promoted β_2AR internalization compared with control siRNA-treated cells (data not shown) (19).

To evaluate whether ARRDC3 regulates agonist-promoted β_2AR degradation, we analyzed β_2AR levels using the radiolabeled antagonist [^{125}I]iodocyanopindolol (25). We found that ARRDC3 overexpression had no effect on β_2AR degradation over a 26-h time course (Fig. 4*C*). This was supported by fixed-cell immunostaining, which revealed a minimal degree of agonist-promoted co-localization of β_2AR and LAMP1 with or without ARRDC3 overexpression following a 4-h agonist treatment (Fig. 4*D*). Thus, ARRDC3 does not appear to regulate endocytosis or degradation of the β_2AR.

We next transiently transfected ARRDC3 in the stable β_2AR cell line and used flow cytometric analysis (24) to evaluate whether ARRDC3 affected the recycling of the internalized β_2AR. As expected, the β_2AR rapidly recycled back to the plasma membrane in control cells, and this also occurred in cells transfected with ARRDC3-AASA/AALA. However, the rate and extent of β_2AR recycling was significantly delayed in cells overexpressing ARRDC3 (Fig. 4*E*). To further characterize the potential effect of ARRDC3 on β_2AR recycling, we used fixed cell immunofluorescence microscopy. We found that the β_2AR co-localized with ARRDC3 on endocytic vesicles after a 20-min treatment with ISO followed by a 30-min agonist washout (Fig. 4*F*). However, under the same conditions, the β_2AR had fully recycled back to the plasma membrane in both vector control and ARRDC3-AASA/AALA-expressing cells (Fig. 4*F*). Importantly, to assess whether endogenous ARRDC3 regulates β_2AR recycling, we used the same flow cytometric analysis and found that knocking down endogenous ARRDC3 resulted in a significantly enhanced rate of β_2AR recycling compared with control siRNA-treated cells (Fig. 4*G*). In addition, we also depleted endogenous ARRDC3 in an SpH-β_2AR-stable HEK293 cell line and monitored the rate of β_2AR recycling in living cells. The SpH tag is pH-sensitive and only fluorescent in a neutral pH, thus providing a way of monitoring cell surface receptor levels. Indeed, depletion of endogenous ARRDC3 resulted in an enhanced rate of β_2AR recycling compared with control siRNA-treated cells (Fig. 4*H*). Taken together, our results demonstrate that ARRDC3 regulates β_2AR recycling but has no significant effect on β_2AR endocytosis or degradation.

We also addressed the question of whether ARRDC3 plays a specific role in β_2AR recycling or might more broadly regulate endosomal recycling. For these studies, we transiently transfected vector or ARRDC3 in HEK293 cells and monitored transferrin receptor (TfR) recycling. Similar to the β_2AR, the TfR recycles via early endosomes, although it is generally viewed as utilizing a different pathway compared with the β_2AR (26). Our data show that ARRDC3 overexpression does not alter the rate of TfR recycling compared with control transfected cells (Fig. 4*I*). This suggests that ARRDC3 plays a specific role in β_2AR recycling and does not broadly disrupt the recycling machinery.

ARRDC3 Promotes β_2AR Retention on EEA1-positive Endosomes by Negatively Regulating Tubule Entry—Because ARRDC3 promoted the retention of β_2ARs on endocytic vesicles (Fig. 4*F*), we further investigated the population of endosomes where the β_2AR was localized. In ARRDC3-overexpressing cells, β_2AR co-localized with ARRDC3 upon 20 min of ISO stimulation followed by a 30-min agonist washout. Furthermore, ARRDC3 and the β_2AR co-localized with EEA1 with little co-localization with LAMP1 or giantin (Fig. 5*A*). This demonstrates that ARRDC3 promotes the retention of β_2AR on EEA1-positive early endosomes.

β_2AR recycling is a highly regulated process. The basic mechanism is thought to involve interaction of a C-terminal PDZ-binding motif on the β_2AR with the PDZ domain in SNX27. SNX27 is associated with Vps26, a component of the retromer complex, and mediates localization of the β_2AR on tubules (26). The internalized β_2AR is recycled through these EEA1-positive early endosomal tubules, which can be visualized in living cells (27). We hypothesized that ARRDC3 delays β_2AR recycling by regulating β_2AR entry into endosomal tubules. To test this, we overexpressed GFP-ARRDC3 in the stable β_2AR HEK293 line, labeled the receptor with fluorescently conjugated FLAG antibody, stimulated cells with ISO for 10 min, and then collected Z-stack images of the cells. An example of β_2AR containing early endosomes with a recycling tubule is shown (Fig. 5*B*). We sampled over 150 β_2AR-containing endosomes with various levels of ARRDC3 (from 1 to >20-fold overexpression based on relative levels of GFP expression). Interestingly, as the concentration of ARRDC3 on these endosomes increased, the number of β_2AR-containing endosomal tubules decreased (Fig. 5*B*). Importantly, this effect was observed at relatively low levels of ARRDC3 expression and was maximal at 4–8-fold overexpression. This suggests that ARRDC3 negatively regulates β_2AR entry into recycling tubules.

Overexpression of ARRDC3 Decreases the Degree of Co-localization of β_2AR and SNX27 on Endosomes—The β_2AR contains a PDZ-binding motif at the distal end of its C-tail (28, 29) that interacts with the PDZ domain of SNX27, an interaction that is crucial for β_2AR recycling (30). In addition, interaction between SNX27 and VPS26 on endosomes has been shown to be critical for the recycling of PDZ-binding motif-containing GPCRs (31, 32). We evaluated whether ARRDC3 plays a role in regulating these two important protein-protein interactions by analyzing the degree of co-localization of β_2AR/SNX27 and SNX27/VPS26 using fixed-cell confocal immunofluorescence microscopy. After 20 min of ISO stimulation, the β_2AR internalized and co-localized with SNX27 on endosomes (Fig. 6*A*, *top left*). Agonist washout led to β_2AR recycling and a decreased level of co-localization with SNX27 over time. Interestingly, in ARRDC3-overexpressing cells, significantly less co-localization was observed between β_2AR and SNX27 upon ISO stimulation and washout (Fig. 6*A*), suggesting that ARRDC3 inhibits the co-localization of β_2AR and SNX27 on endosomes. In contrast, ARRDC3 overexpression did not affect the degree of co-localization between SNX27 and VPS26 (Fig. 6*B*).

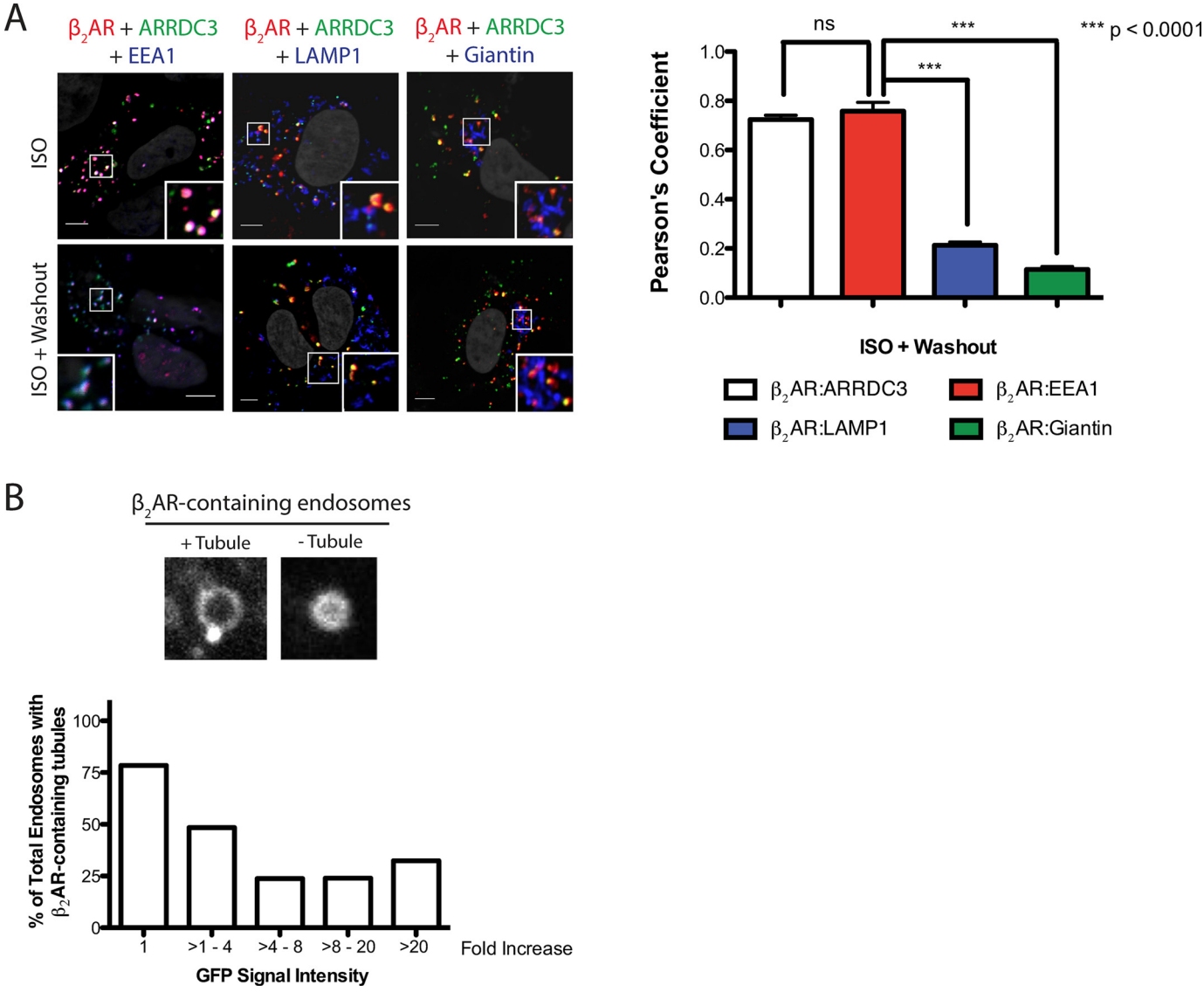

FIGURE 5. **ARRDC3 retains the β_2AR on EEA1-positive endosomes and negatively regulates β_2AR tubule entry.** *A,* representative images and corresponding quantifications of the co-localization of the β_2AR, ARRDC3, and endocytic markers upon 20 min of treatment with 10 μM ISO followed by 25 min of treatment with 10 μM propranolol. Unpaired *t* test. Pearson's coefficients are the mean ± S.E. from $n = 30$. *B,* representative β_2AR-containing endosomes ± tubules are shown. Percentages of total β_2AR-containing endosomal tubules were assessed in cells with various levels of pEGFP-ARRDC3 expression (n = 20–40 at each expression level). *Scale bars,* 5 μm.

We also evaluated the localization of β_2AR, ARRDC3, and SNX27 on endosomes in living cells. After 10 min of ISO stimulation, cell surface-labeled and internalized β_2AR could be visualized on the body and tubule of enlarged and lumen-hollowed early endosomes. mApple-SNX27 was concentrated at either the base of or on endosomal tubules and co-localized with the β_2AR (Fig. 6*C*). In contrast, in GFP-ARRDC3-expressing cells, the β_2AR co-localized with ARRDC3 but did not co-localize with mApple-SNX27. Furthermore, although β_2AR, ARRDC3, and SNX27 could be visualized on the same endosomes, the β_2AR-ARRDC3 complex was more prominently localized to the endosomal body as opposed to a tubule, where SNX27 mainly resided (Fig. 6*C*). Taken together, our data suggest that ARRDC3 interacts with the β_2AR on endosomes and inhibits receptor localization with SNX27 on endosomal tubules.

ARRDC3 Regulates β_2AR Signaling on Endosomes—The concept of acute β_2AR-dependent signal transduction on endosomes has been directly demonstrated recently (6). Because ARRDC3 modulates the endosomal level of β_2AR by regulating β_2AR recycling, we tested whether ARRDC3 affected acute β_2AR-dependent signal transduction on endosomes. Using a previously described luminescent-based assay to monitor cAMP production in living cells in real time (33), we found that the overall β_2AR-dependent cAMP production was increased in ARRDC3-expressing cells upon ISO stimulation, compared with control cells (Fig. 7*A*). To determine whether this increase was due to cAMP production from endosomes, the cells were treated with Dyngo-4a, a dynamin inhibitor that blocks β_2AR endocytosis (6), prior to ISO stimulation. Dyngo-4a treatment resulted in an 11.4 ± 1.9% decrease in ISO-stimulated cAMP production in control

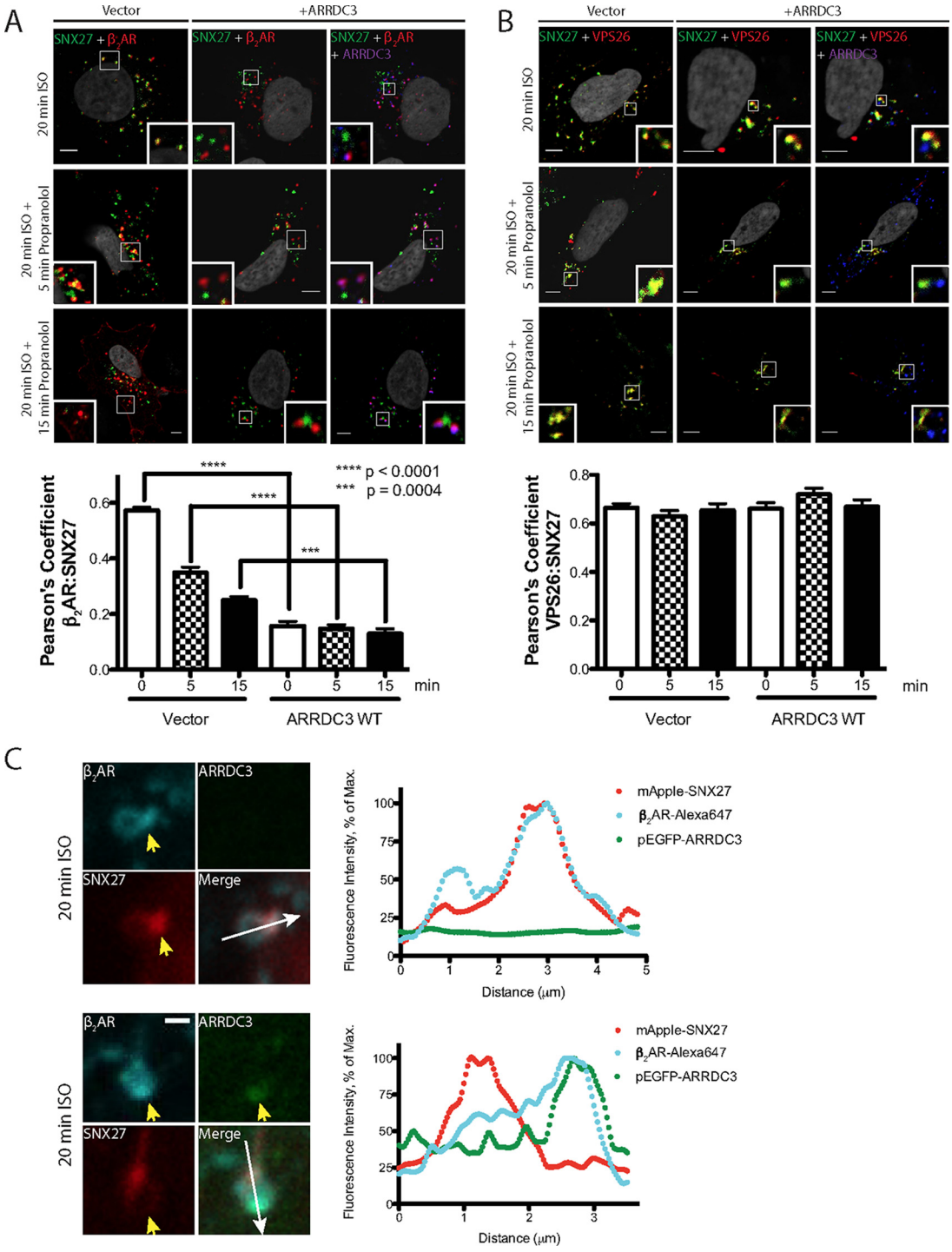

FIGURE 6. **Overexpression of ARRDC3 decreases the co-localization of the β_2AR and SNX27 on endosomes.** *A,* representative images and corresponding quantifications of β_2AR localization with endogenous SNX27 in cells with or without ARRDC3 overexpression were analyzed by immunofluorescence staining upon 20 min of treatment with 10 μM ISO followed by 10 μM propranolol treatment for the indicated times. Three independent experiments were performed. Pearson's coefficients are the mean ± S.E. and compared using an unpaired *t* test ($n = 30$). *Scale bars,* 5 μm. *B,* representative images and corresponding quantifications of the localization of endogenous SNX27 and VPS26 in cells with or without ARRDC3 overexpression were analyzed by immunofluorescence staining upon 20 min of treatment with 10 μM ISO followed by 10 μM propranolol treatment for the indicated times. Three independent experiments were performed. Pearson's coefficients are the mean ± S.E. and compared using an unpaired *t* test ($n = 30$). *Scale bars,* 5 μm. *C,* representative immunofluorescence confocal live cell images and corresponding line scan analysis are shown to demonstrate the localization of the β_2AR, pEGFP-ARRDC3, and mApple-SNX27 on the same endosomes. FLAG-β_2AR-stable HEK293 cells were transiently transfected with mApple-SNX27 and vector/pEGFP-ARRDC3. Three independent experiments were performed, and over 50 endosomes were examined. *Scale bars,* 1 μm.

cells suggesting some contribution of endosome-localized activation of β_2AR-mediated Gα_s activity (Fig. 7, *B–D*) (6). By comparison, there was a 32.4 ± 3.3% decrease in cAMP production in ARRDC3-transfected cells upon Dyngo-4a treatment, suggesting that ARRDC3 significantly enhances the level of β_2AR-mediated cAMP production on endosomes

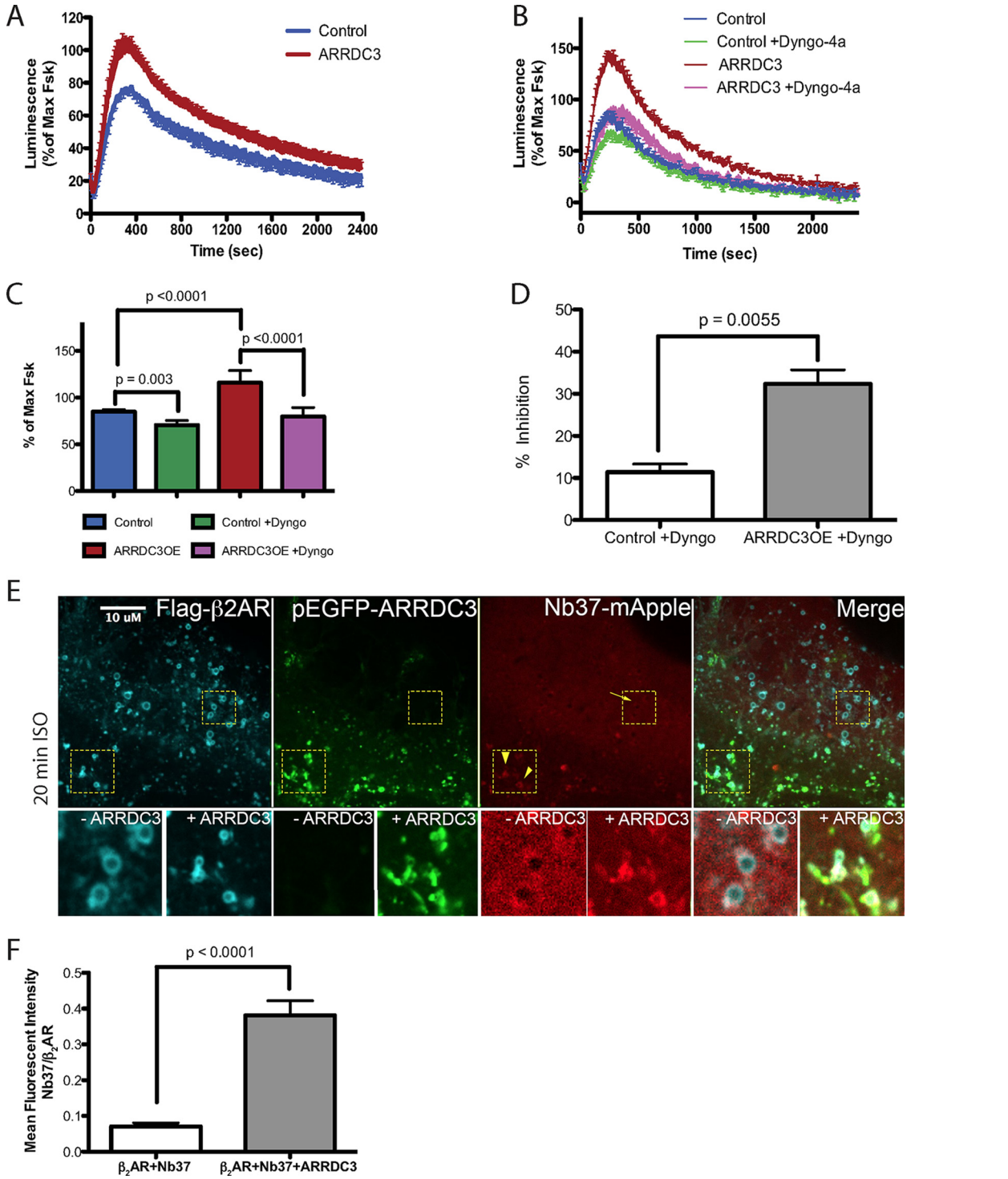

FIGURE 7. **ARRDC3 modulates β_2AR-dependent Gα_s protein-mediated signal transduction on endosomes.** *A,* forskolin-normalized β_2AR-mediated cAMP response in cells with or without ARRDC3 overexpression. More than six independent experiments were performed. Representative experimental data are shown. *B,* forskolin-normalized β_2AR-mediated cAMP response in the absence or presence of 30 μM Dyngo-4a in cells with or without ARRDC3 expression. Four independent experiments were performed. Representative experimental data are shown. *C,* average of 10 consecutive maximum values of each condition in *B*. The *graph* represents the mean ± S.E. from four independent experiments. Unpaired *t* test. *D,* calculated by using numerical values from *C*. % of inhibition = (1 − (maximum value of control or ARRDC3 + Dyngo/maximum value of control or ARRDC3)) × 100. The *graph* represents the mean ± S.E. from the four independent experiments in *C*. Unpaired *t* test. *E,* representative confocal live cell images and co-localization analysis of HEK293 cells overexpressing pEGFP-ARRDC3 and Nb37-mApple. Cells were stimulated with 10 μM ISO for 20 min. $n = 11$. *F,* fluorescent intensity of Nb37-mApple on β_2AR-occupied early endosomes in the presence or absence of pEGFP-ARRDC3. The *graph* represents the mean ± S.E. from >50 endosomes for each condition. Unpaired *t* test.

(Fig. 7, *B–D*). Furthermore, we monitored the recruitment of mApple-Nb37, a nanobody biosensor that recognizes the catalytic intermediate of Gα_s protein activation (6), and we found that ARRDC3 expression significantly enhances the level of active Gα_s on endosomes compared with control cells (Fig. 7, *E* and *F*). Taken together, we conclude that

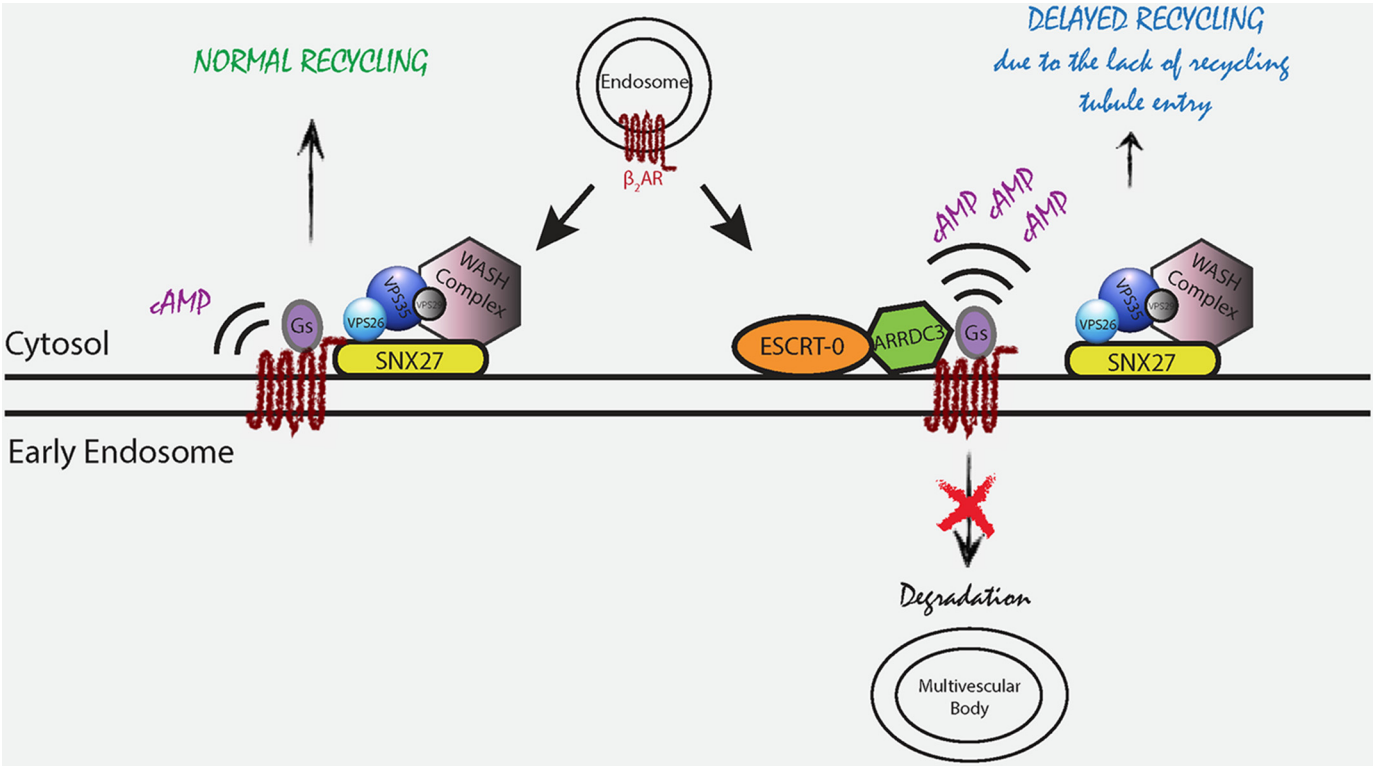

FIGURE 8. **Model of ARRDC3 regulation of β_2AR trafficking and endosomal signaling.** ARRDC3 is primarily localized to EEA1-positive early endosomes, where it interacts with the ESCRT-0 complex. When ARRDC3 is not present, internalized β_2AR interacts with SNX27 on early endosomes and undergoes rapid recycling. When ARRDC3 is present on endosomes, it associates with the internalized β_2AR, retains it on early endosomes, and delays β_2AR recycling by inhibiting its entry into SNX27-occupied endosomal recycling tubules. In turn, ARRDC3 modulates β_2AR-dependent Gα_s-mediated cAMP production on endosomes.

ARRDC3 regulates acute β_2AR-dependent Gα_s-mediated cAMP production on endosomes.

Discussion

We show that ARRDC3 is primarily localized to EEA1-positive early endosomes, where it interacts with STAM-1, a component of the ESCRT-0 complex. Functionally, ARRDC3 retains internalized β_2ARs on EEA1-positive early endosomes and delays β_2AR recycling by directly interacting with the receptor and preventing it from associating with SNX27-occupied endosomal recycling tubules. This results in ARRDC3 modulation of β_2AR-dependent Gα_s-mediated cAMP production on endosomes (Fig. 8).

Although previous studies suggested that ARRDC3 localizes to both the plasma membrane and endocytic vesicles, these observations were made in heterologous cell lines overexpressing ARRDC3 (15, 19, 34, 35). Using fixed-cell confocal immunofluorescence microscopy, we demonstrated that both overexpressed (Fig. 1*B*) and endogenous (Fig. 1*D*) ARRDC3 are primarily localized to EEA1-positive early endosomes. Plasma membrane-localized ARRDC3 was only detected when pEGFP-ARRDC3 was highly overexpressed (data not shown), and no endogenous ARRDC3 was detected at the plasma membrane of BT549 cells (Fig. 1*D*). Although our studies suggest that ARRDC3 is primarily localized at EEA1-positive early endosomes in HEK293 and BT549 cells, it's worth noting that Dores *et al.* (35) found that overexpressed ARRDC3 was equally distributed on both early and late endosomes in HeLa cells. Thus, it appears that the cellular localization of ARRDC3 is dependent on both the cell type and expression level.

Previous studies, as well as our own, show that ARRDC3 is mainly localized to the plasma membrane when both PP*X*Y motifs of ARRDC3 are mutated to AA*X*A (15, 19) (Fig. 1*A*), although we found that only a single PP*X*Y motif is necessary for endosomal localization (Fig. 2*C*). We further found that the C-tail of ARRDC3 alone did not exhibit any specific localization to cellular compartments (Fig. 2*C*), suggesting that the PP*X*Y motifs and arrestin domains of ARRDC3 are necessary to localize it to EEA1-positive early endosomes. Recently, the crystal structure of the N-domain of ARRDC3 has been solved (36). Interestingly, the residues on the concave surface of the N-domain are highly basic and were bound to phosphate ions in the crystal. These basic residues might interact with phosphoinositides, such as phosphatidylinositol 4,5-bisphosphate and phosphatidylinositol 3-phosphate, present on the plasma membrane and endosomal membrane, respectively, thus facilitating ARRDC3 localization to membranes. Another potential contributor to ARRDC3 localization is ubiquitination because the ubiquitination state of ARRDC3 correlates with its endosomal localization (Fig. 2*D*). The observation that ARRDC3 is ubiquitinated was not surprising because it interacts with the HECT-domain E3 ubiquitin ligases via its PP*X*Y motifs (15, 18, 19). Interestingly, although ARRDC3 interacts with the ESCRT-0 complex on EEA1-positive early endosomes (19), ARRDC3-AASA/AALA does not. Because both HRS and STAM contain ubiquitin-interacting motifs (20), it is possible

that ARRDC3 localizes to early endosomes by interacting with the ubiquitin-interacting motifs of HRS and STAM via its poly-ubiquitinated moieties. Interestingly, the expression level of ARRDC3 noticeably increased when co-expressed with STAM-1 (Fig. 2*A*) suggesting that STAM-1 may regulate the stability of ARRDC3. Thus, we speculate that the basic residues on the concave surface of the arrestin domains of ARRDC3 facilitate the membrane localization of ARRDC3 by interacting with phosphoinositides, although the poly-ubiquitinated moiety of ARRDC3 specifically localizes it to early endosomes by interacting with the ESCRT-0 complex.

Previous co-immunoprecipitation studies suggested that ARRDC3 interacts with the β_2AR (15, 19, 36, 37), and one study reported that this interaction was agonist-dependent (15). We used three approaches to assess ARRDC3 interaction with the β_2AR, co-immunoprecipitation, BRET, and a pulldown assay using *in vitro* translated ARRDC3 and purified β_2AR. Our results demonstrate that ARRDC3 and the β_2AR interact in a ligand-independent manner and our BRET results suggest that this interaction is direct (Fig. 3). Although the interaction of these proteins is ligand-independent, there is a clear agonist-dependent component to the interaction because agonist-dependent endocytosis of the β_2AR is required to mediate the co-localization of the β_2AR with ARRDC3 as noted previously by Han *et al.* (19) (Fig. 4).

Although we know relatively little about how ARRDC3 interacts with the β_2AR, previous studies identified several basic residues on the ARRDC3 arrestin-like domains that appear to contribute to this process (36). Although one might speculate that ARRDC3 would interact with the β_2AR in a manner similar to β-arrestin interaction with GPCRs, our results suggest that the β_2AR does not need to undergo an agonist-promoted conformational change to interact with ARRDC3. Moreover, computer-modeling studies and sequence comparisons suggest that ARRDC3 likely does not contain a polar core (12), a region that is critical for proper interaction of β-arrestin with the phosphorylated β_2AR. Thus, we believe that the interaction between ARRDC3 and the β_2AR is not driven by agonist stimulation or by the phosphorylation state of the receptor.

The functional role of ARRDC3 in β_2AR endocytic trafficking is controversial (15, 19), and the specific mechanism by which it regulates trafficking has not been elucidated. We found that ARRDC3 regulates the β_2AR endosomal residence time (Fig. 4, *E–H*) by modulating β_2AR and SNX27 co-localization (Fig. 6, *A* and *C*) and subsequent entry into endosomal tubules (Fig. 5*B*). However, ARRDC3 does not function to regulate β_2AR endocytosis (Fig. 4, *A* and *B*) or degradation (Fig. 4, *C* and *D*). Although it seems likely that ARRDC3 association with the ESCRT-0 machinery and the β_2AR may hinder receptor binding to SNX27, we cannot exclude the possible involvement of other proteins in this process. For example, ARRDC2 and ARRDC4 have also been shown to co-localize with the β_2AR on endosomes (19). Moreover, ARRDC3 has been suggested to homodimerize and heterodimerize with other ARRDCs and β-arrestins (38). Although we did not dissect the functional roles of other ARRDCs in β_2AR recycling in this study, it is possible that they may have additional roles in GPCR sorting and/or working together with ARRDC3.

Recently, SNX27 as well as the retromer complex have been shown to regulate the recycling of PDZ-binding motif-containing GPCRs (31, 32). Because ARRDC3 regulates β_2AR recycling by directly interacting with the β_2AR and possibly modulating the association of SNX27 with the PDZ-binding motif on the C-tail of the β_2AR (30), it is possible that interaction between ARRDC3 and other GPCRs may play a broad role in regulating receptor sorting.

Once the interaction between the β_2AR and SNX27 is disrupted, the β_2AR is degraded via the endosome-lysosome pathway instead of recycling back to the plasma membrane (30). Interestingly, although our data suggest that ARRDC3 prevents the interaction between the β_2AR and SNX27 (Fig. 6), the rate of β_2AR degradation was unaffected by ARRDC3 (Fig. 4, *C* and *D*). It is possible that ARRDC3 also influences receptor association with the ESCRT complex, thus "retaining" the β_2AR on endosomes. Furthermore, because β_2AR degradation is influenced by its ubiquitination state, which is mediated by β-arrestin interaction with Nedd4 (39–41), ARRDC3 might play a role in regulating ubiquitination/deubiquitination of the β_2AR on endosomes, thereby preventing the receptor from entering the endosome-lysosomal pathway. Finally, it will also be interesting to evaluate whether ARRDC3 regulates the degradation of GPCRs that normally undergo rapid degradation upon endocytosis. Although this remains to be investigated, a recent study demonstrated that ARRDC3 can regulate the lysosomal sorting of PAR1 via its ability to promote ubiquitination of ALIX, a protein that directly binds to some GPCRs to mediate lysosomal sorting (35). Thus, ARRDC3 may have a diverse role in regulating GPCR sorting.

By actively retaining the β_2AR on endosomes, ARRDC3 regulates acute β_2AR-dependent Gα_s-mediated cAMP production in living cells (Fig. 7). It has been recently suggested that location-specific signaling events are able to elicit discrete downstream consequences that are distinct from receptor-mediated signaling on the plasma membrane. For example, β_2AR-dependent Gα_s-mediated endosome signaling has been shown to specifically modulate the activation of cAMP-dependent genes (42). It will be interesting to evaluate whether ARRDC3 also regulates this process and/or has different downstream consequences.

In summary, we found that ARRDC3 is primarily localized to early endosomes, where it interacts with and retains internalized β_2AR, thereby preventing β_2AR entry into SNX27-occupied endosome tubules. As a result, ARRDC3 delays β_2AR recycling and modulates β_2AR-dependent signal transduction on endosomes.

Experimental Procedures

Reagents—The sense-strand silencing siRNA sequence for ARRDC3 is 5′-CGAAAGAGAUGAUGAUAAU(dTdT)-3′. Antibodies used include the following: rabbit polyclonal ARRDC3 antibody (Abcam, ab64817, 1:500); mouse monoclonal anti-FLAG® antibody (clone M1, Sigma, F3040, 1 μg/ml, and clone M2, Sigma, F3165, 1 μg/ml); rabbit polyclonal anti-FLAG® antibody (Sigma, F7425, 1:1000); mouse monoclonal EEA1 antibody (clone 14/EEA1, BD Biosciences, 610456, 1:1000); mouse monoclonal SNX27 antibody (clone 1C6,

Abcam, ab77799, 1:500); rabbit polyclonal VPS26 antibody (Abcam, ab23892, 1:500); rabbit polyclonal STAM antibody (ProteinTech™, 12434-1-AP, 1:25 (immunofluorescence), 1:1000 (Western blot)); mouse monoclonal GFP antibody (Santa Cruz Biotechnology, sc-9996, 1:2000); mouse monoclonal HA.11 antibody (clone 16B12, Covance, MMS-101P, 1:1000); mouse monoclonal ubiquitin antibody (clone P4D1, Cell Signaling, 3936, 1:1000); mouse monoclonal LAMP1 antibody (clone H4A3, DSHB, 1:1000); and rabbit polyclonal giantin antibody (Covance, PRB-114C, 1:500). mApple-SNX27 was provided by B. T. Lobingier in the laboratory of M. von Zastrow, and GFP10-β-arrestin2 and β_2AR-RlucII were provided by M. Bouvier, and FLAG-STAM1 was provided by A. Marchese.

Cell Culture and Transfection—Human embryonic kidney 293 (HEK293) cells were maintained in Dulbecco's modified Eagle's Medium (DMEM) (Fisher) supplemented with 10% fetal bovine serum (FBS) (Invitrogen) and 10 mM HEPES (Fisher). FLAG-β_2AR-stable HEK293 cells were maintained in DMEM supplemented with 10% FBS, 10 mM HEPES, and 500 μg/ml G418 (Fisher). BT549 cells were maintained in RPMI 1640 medium with L-glutamine and 25 mM HEPES (Fisher) supplemented with 10% FBS. HEK293 and BT549 cells grown to ~70% confluence in 10-cm plates were transiently transfected with 6 μg of total plasmid DNA using XtremeGene HP (Roche Applied Science) or 20 nM siRNA using Lipofectamine 2000 (Invitrogen) for 48 h.

Co-immunoprecipitation—48 h post-transfection, cells were serum-starved for 1 h, stimulated with vehicle or 10 μM ISO for 20 min at 37 °C, washed with ice-cold phosphate-buffered saline (PBS), and then lysed in buffer containing 50 mM Tris-HCl, pH 7.5, 150 mM NaCl, 1% Triton X-100, 1 mM phenylmethylsulfonyl fluoride, 5 mM EDTA, protease inhibitor mixture, and PhosStop tablet (Roche Applied Science). Cells were sonicated and centrifuged at 3000 rpm for 10 min at 4 °C, and protein concentrations of the supernatant were determined using a Bradford protein assay (Bio-Rad). Equal amounts of the soluble lysate were immunoprecipitated with a polyclonal anti-FLAG antibody (Sigma) and protein A-agarose beads (Roche Applied Science) at 4 °C overnight or at room temperature for 2 h. Immunoprecipitates and total cell lysates were separated by SDS-PAGE, transferred to nitrocellulose, and immunoblotted with appropriate antibodies. Immunoblots were incubated with SuperSignal West Pico reagent (Pierce), exposed to film, and developed.

To detect polyubiquitinated ARRDC3, cells were lysed in 50 mM HEPES, pH 7.5, 0.5% Nonidet P-40, 250 mM NaCl, 2 mM EDTA, 10% (v/v) glycerol, 1 mM sodium orthovanadate, 1 mM sodium fluoride, 1 mM phenylmethylsulfonyl fluoride, 1 mM *N*-ethylmaleimide, 1 protease inhibitor tablet (Roche Applied Science), and 1 PhosStop tablet (Roche Applied Science) and centrifuged at 3000 rpm for 10 min at 4 °C. Equal amounts of the soluble lysate were immunoprecipitated with an ARRDC3 antibody (Abcam) and protein A-agarose beads (Roche Applied Science) at 4 °C for 4 h. Samples were washed three times with lysis buffer, and bound protein was eluted with 2× SDS sample buffer.

Bioluminescence Resonance Energy Transfer (BRET)—24 h post-transfection, cells were plated in poly-L-ornithine (Sigma)-coated opaque 96-well plates (Optiplate, PerkinElmer Life Sciences) at a density of 100,000 cells per well in DMEM with high glucose (Invitrogen). After 24 h of incubation at 37 °C, cells were washed three times with PBS + glucose (Invitrogen), and 2.5 μM coelenterazine 400a was added to each well. BRET was measured at 510 nm following addition of indicated ligands using a Tecan Infinite F500 microplate reader. BRET ratios = (light emitted by GFP10)/(light emitted by RLucII). ΔBRET = BRET ratio of stimulated trials − BRET ratio of unstimulated trials.

Expression and Purification of β_2AR—The full-length β_2AR was cloned into pVL1392 transfer vector for Bestbac expression system (Expression Systems Inc.). The recombinant baculovirus was used to infect Sf9 cells, and the infected cells were harvested after 48 h of incubation at 27 °C as described previously (43). Cell pellets were lysed by stirring in lysis buffer (20 mM HEPES, pH 7.5, 5 mM EDTA, 1 μM alprenolol) supplemented with protease inhibitors (Roche Applied Science) for 30 min. The receptor was extracted from the cell membrane using Dounce homogenization in solubilization buffer (20 mM HEPES, pH 7.5, 100 mM NaCl, 1% dodecyl maltoside, 1 μM alprenolol) supplemented with protease inhibitors for 1 h at room temperature. After further addition of 2 mM $CaCl_2$, the solubilized receptor was clarified by high speed centrifugation at 18,000 × *g* for 30 min. The receptor bearing N-terminal FLAG epitope was captured by M1 antibody affinity chromatography (Sigma) and then eluted with HMS-CHS buffer (20 mM HEPES, pH 7.5, 350 mM NaCl, 0.1% dodecyl maltoside, 0.01% cholesterol hemisuccinate) supplemented with 5 mM EDTA and 200 μg/ml free FLAG peptide. The protein sample was further purified by affinity chromatography using alprenolol-Sepharose to select functional receptors (44). Size-exclusion chromatography with Superdex-200 column (GE Healthcare) equilibrated in HMS-CHS buffer was used as a final purification step. The receptor was concentrated to ~150 μM and used in subsequent studies. The purity of β_2AR was >95% as assessed by SDS-PAGE.

In Vitro Pulldown Assay—Purified β_2AR (~0.8 μM) was incubated with 500 μM ISO or 400 μM propranolol in assay buffer (20 mM Tris, pH 7.5, 2 5 mM NaCl, 1 mM $CaCl_2$, 0.0001% maltose-neopentyl glycol) for 30 min on ice. The mixture was then incubated with anti-FLAG M1-agarose beads (Sigma) for 45 min at 4 °C followed by three washes with assay buffer. The receptor-bound beads were then incubated with *in vitro* translated ^{35}S-labeled ARRDC3 in assay buffer containing the appropriate ligand for 45 min at 4 °C with rotation, washed three times with assay buffer, and then incubated with elution buffer (100 mM glycine, pH 3.5, 0.01% maltose-neopentyl glycol) for 30 min on ice and centrifuged. Supernatant was collected and analyzed by fluorography. *In vitro* translated ^{35}S-labeled ARRDC3 was generated using TnT®-coupled reticulocyte lysate system (Promega). Amplify™ (GE Healthcare) was used to enhance the fluorographic signal.

Analysis of Receptor Internalization Using Cell Surface ELISA—48 h post-transfection, FLAG-β_2AR-stable HEK293 cells were serum-starved, stimulated with 10 μM ISO for the indicated times at 37 °C, washed with ice-cold PBS, and fixed with 4% paraformaldehyde on ice. The amount of remaining

cell surface FLAG-β_2AR was determined by incubating with M1 anti-FLAG antibody (Sigma) and washing and incubating with an HRP-conjugated horse anti-mouse secondary antibody (Vector Laboratories). After washing, cells were incubated with one-step ABTS (Pierce); an aliquot was removed, and absorbance at 405 nm was determined.

Analysis of Receptor Internalization Using Flow Cytometry—48 h post-transfection, FLAG-β_2AR-stable HEK293 cells were incubated with M1 FLAG antibody conjugated to Alexa647 in DMEM supplemented with 1 mM $CaCl_2$ for 15 min to label cell surface FLAG-tagged receptor. Cells were washed once with DMEM/$CaCl_2$ and then treated with 10 μM ISO for 20 min. To stop the stimulation, cells were placed on ice and washed once with ice-cold PBS/EDTA. 250 μl of ice-cold PBS/EDTA were added to each sample and shaken at 4 °C for 15 min. Cells were transferred into tubes and analyzed by flow cytometry.

Receptor Degradation Assay—24 h post-transfection, equal amounts of cells were plated onto 6-well dishes. The next day, cells were treated with either vehicle or 10 μM (−)-isoproterenol in 0.1 mM ascorbic acid for the indicated times. At each time point, cells were washed four times with PBS, then lysed by addition of lysis buffer (20 mM Tris-HCl, pH 7.5, 2 mM EGTA, 5 mM EDTA, and 1 complete protease inhibitor tablet (Roche Applied Science)), and sonicated on ice. Samples were centrifuged in a tabletop centrifuge at 13,000 rpm for 10 min at 4 °C. Receptor expression was measured in the cell lysate by incubating with 1 nM [^{125}I]iodocyanopindolol (PerkinElmer Life Sciences) ± 10 μM propranolol at room temperature for 1 h. Binding reactions were terminated by the addition of 5× 4 ml of ice-cold wash buffer (25 mM Tris-HCl, pH 7.5, 2 mM $MgCl_2$) followed by rapid filtration through Whatman GF/C filters using a Brandel Cell Harvester. [^{125}I]Iodocyanopindolol binding was quantitated by gamma emission counting.

Analysis of Receptor Recycling Using Flow Cytometry—48 h post-transfection, FLAG-β_2AR-stable HEK293 cells were incubated with M1 FLAG antibody (Sigma) in DMEM supplemented with 1 mM $CaCl_2$ for 15 min to label cell surface FLAG-tagged receptors. Cells were washed once with DMEM/$CaCl_2$ and then treated with 10 μM ISO for 25 min to drive labeled β_2AR to steady state in the endocytic pathway (surface labeling assay). Alternatively, cells were incubated with 10 μM ISO plus M1 FLAG antibody conjugated to Alexa647 (M1 FLAG-Alexa647; 1 μg/ml) in DMEM supplemented with 1 mM $CaCl_2$ for 25 min (feeding assay). Any antibody-labeled FLAG-β_2AR remaining on the cell surface was then stripped by washing the cells with ice-cold PBS/EDTA three times. Cells were then treated with 10 μM propranolol in DMEM supplemented with 1 mM $CaCl_2$ for the indicated times, placed on ice to stop β_2AR trafficking, and removed from the plate with ice-cold staining buffer (PBS, $CaCl_2$, 1% BSA). Cells were either transferred into flow cytometry tubes for analysis (feeding assay) or incubated with anti-mouse-Alexa488 (Molecular Probes) in staining buffer on ice for 1 h and then washed three times with staining buffer. The amount of recycled cell surface FLAG-β_2AR at each time point was measured using a FACSCalibur Flow Cytometer (BD Biosciences).

Analysis of Receptor Recycling in Living Cells—48 h post-transfection, cells were imaged live at 37 °C with 20 × 0.75 numerical aperture (NA) objective under wide-field illumination in Opti-MEM (Invitrogen) supplemented with 10% FBS and 40 mM HEPES, pH 7.5. Images were collected at 1-min intervals, and four time points were collected before ISO addition. Cells were stimulated with 10 μM ISO for 15 min; ISO-containing medium was then removed; cells were washed once with plain medium and medium containing 10 μM alprenolol (Sigma) was added and incubated for 20 min. Measured intensities were background-corrected and normalized to the average of the first four frames.

Fixed-cell Immunofluorescence Microscopy—To assess the cellular localization of ARRDC3, β_2AR, and SNX27/VPS26 after agonist washout, FLAG-β_2AR-stable HEK293 cells were transiently transfected with either pEGFP-ARRDC3 or vector control. 48 h post-transfection, cells were incubated with M1 anti-FLAG antibody for 20 min to selectively label β_2AR present in the plasma membrane. Cells were then stimulated with 10 μM ISO for 20 min, quickly washed three times with ice-cold PBS/EDTA, and incubated with 10 μM propranolol in DMEM for the indicated times at 37 °C.

To assess the cellular localization of ARRDC3 and endocytic markers, cells were transiently transfected with either pEGFP-ARRDC3/vector control (HEK293 cells) or siARRDC3/siControl (BT549 cells). To study the localization of pEGFP-ARRDC3, 48 h post-transfection, cells were fixed with 2% paraformaldehyde (Sigma)/PBS for 10 min at room temperature, washed once with PBS and incubated in blocking buffer (0.1% Triton X-100, 1% BSA, 10% goat serum, 1 mM $CaCl_2$, PBS) for 1 h at room temperature. To study the localization of endogenous ARRDC3 in BT549 cells, 48 h post-transfection, cells were fixed with 3.7% paraformaldehyde/PHEM (60 mM PIPES, 25 mM HEPES, 10 mM EGTA, 2 mM $MgCl_2$, pH 7.2) for 10 min at room temperature, washed once with PHEM, and incubated in blocking buffer (0.1% saponin, 10% goat serum, 3% BSA, PHEM) for 1 h at room temperature. Cells were then probed with appropriate primary antibodies, washed four times with 0.05% Triton X-100/PBS or 0.05% saponin/PHEM, re-blocked with appropriate blocking buffer for 30 min at room temperature, and then probed with secondary antibodies for 1 h at room temperature. After secondary antibody staining, cells were washed four times and mounted with ProLong Diamond mounting medium (Invitrogen). Laser-scanning confocal microscopy was performed using a microscope (LSM510, Carl Zeiss, Inc.) fitted with a ×63/NA 1.4 oil objective lens. Although the overexpression of ARRDC3 in HEK293 cells was <10-fold over endogenous levels (data not shown), we typically only analyzed cells with relatively low amounts of expressed pEGFP-ARRDC3 for immunofluorescence microscopy experiments.

Live-cell Imaging—To visualize and analyze β_2AR-containing endosomal tubules, pEGFP-ARRDC3 was transiently transfected in FLAG-β_2AR-stable HEK293 cells. 48 h post-transfection, surface receptors were labeled by incubating cells with M1 anti-FLAG antibody (Sigma) conjugated to Alexa647 (Invitrogen) for 10 min at 37 °C. Cells were washed once with imaging media (Opti-MEM supplemented with 10% FBS and 40 mM HEPES), incubated with 10 μM ISO for 10 min at 37 °C, and then imaged on a Nikon TE-2000E inverted microscope with a

×100 1.49NA TIRF objective (Nikon) and a Yokogawa CSU22 spinning disc confocal head. A 488 nm Ar laser and 568 nm Ar/Kr laser were used as light sources for imaging pEGFP and FLAG signals, respectively. *Z*-stacks of endosomes were taken between 10 and 30 min after agonist addition and exported as TIFF files. Analysis of receptor-containing endosomal tubule formation was carried out using ImageJ (rsb.info.nih.gov) and the Oval Profile plugin. Briefly, endosomes were outlined using the oval tool. Oval Profile was used to carry out a linear fluorescence intensity scan in 60 subsections. The data were exported to Excel where the background was subtracted.

For co-localization of β_2AR, ARRDC3, and SNX27, live cell imaging was performed using Yokagawa CSU22 spinning disk confocal microscope with a ×100, 1.4NA, oil objective, and a CO_2 and 37 °C temperature-controlled incubator. Receptors were surface-labeled by addition of M1 anti-FLAG antibody (1:1000, Sigma) conjugated to Alexa647 to the media for 10 min. ISO was added, and cells were imaged in DMEM without phenol red supplemented with 30 mM HEPES, pH 7.4 (UCSF cell culture facility). Time-lapse images were acquired with a Cascade II EM-charge-coupled device (CCD) camera (Photometrics) driven by Micro-Manager 1.4. Images were saved as 16 bit TIFF files. Quantitative image analysis was carried out on unprocessed images using ImageJ software.

Luminescence-based Rapid cAMP Assay—HEK293 cells were transiently transfected with a plasmid encoding a cyclic-permuted luciferase reporter construct. This reporter construct produces cAMP-dependent activation of luciferase activity in intact cells rapidly and reversibly and is based on a mutated RIIβB cAMP-binding domain from PKA (pGloSensor-20F, Promega). 24 h post-transfection, cells were plated in poly-D-lysine-coated 24-well plates containing ~200,000 cells per well and equilibrated to 37 °C in a light-proof cabinet until cells adhered to the plates. Cells were then equilibrated for 40 min in the presence of 250 μg/ml luciferin (Biogold) in 250 μl of serum and phenol red-free DMEM supplemented with 30 mM HEPES. An image of the plate was focused on a 512 × 512-pixel electron multiplying charge-coupled device sensor (Hamamatsu C9100–13). Luminescence images were collected every 10 s to obtain basal luminescence values. ISO (10 μM) diluted in 250 μl of serum and phenol red-free DMEM supplemented with 30 mM HEPES was then added to desired wells. In endocytic manipulation experiments, cells were pre-incubated with 30 μM Dyngo-4a (Abcam Biochemicals) for 15 min. Sequential images were acquired every 10 s using Micro-Manager, and integrated luminescence intensity detected from each well was calculated after background subtraction and correction using scripts written in MATLAB (MathWorks). As a control, in each multiwell plate, as well as for each experimental condition, a reference value of luminescence was measured in the presence of 5 μM forskolin, a manipulation that stimulates a moderate amount of receptor-independent activation of adenylyl cyclase. The average luminescence value was normalized to the maximum luminescence value measured in the presence of 5 μM forskolin.

Western Blot—Western blots were performed using standard procedures.

Author Contributions—X. T. and J. L. B. designed the overall project. X. T. carried out most of the experiments in the laboratory of J. L. B. X. T., S. L. B., and M. A. P. designed and performed the experiments on the β2AR-containing endosomal tubule formation in the laboratory of M. A. P. R. I. designed and R. I. and X. T. performed the experiments on the β2AR signaling on endosomes in the laboratory of M. v. Z. Y. D. provided purified receptor for binding studies, and all authors contributed to the writing of the manuscript.

Acknowledgments—We thank Drs. B.T. Lobingier, M. Bouvier, and A. Marchese and the Sidney Kimmel Cancer Center Bioimaging Facility for reagents, technical advice, training, and support.

References

1. Hanyaloglu, A. C., and von Zastrow, M. (2008) Regulation of GPCRs by endocytic membrane trafficking and its potential implications. *Annu. Rev. Pharmacol. Toxicol.* **48,** 537–568
2. Neves, S. R., Ram, P. T., and Iyengar, R. (2002) G protein pathways. *Science* **296,** 1636–1639
3. Goodman, O. B., Jr., Krupnick, J. G., Santini, F., Gurevich, V. V., Penn, R. B., Gagnon, A. W., Keen, J. H., and Benovic, J. L. (1996) β-Arrestin acts as a clathrin adaptor in endocytosis of the β2-adrenergic receptor. *Nature* **383,** 447–450
4. Ferguson, S. S., Downey, W. E., 3rd., Colapietro, A. M., Barak, L. S., Ménard, L., and Caron, M. G. (1996) Role of β-arrestin in mediating agonist-promoted G protein-coupled receptor internalization. *Science* **271,** 363–366
5. Kang, D. S., Tian, X., and Benovic, J. L. (2014) Role of β-arrestins and arrestin domain-containing proteins in G protein-coupled receptor trafficking. *Curr. Opin. Cell Biol.* **27,** 63–71
6. Irannejad, R., Tomshine, J. C., Tomshine, J. R., Chevalier, M., Mahoney, J. P., Steyaert, J., Rasmussen, S. G., Sunahara, R. K., El-Samad, H., Huang, B., and von Zastrow, M. (2013) Conformational biosensors reveal GPCR signalling from endosomes. *Nature* **495,** 534–538
7. Calebiro, D., Nikolaev, V. O., Gagliani, M. C., de Filippis, T., Dees, C., Tacchetti, C., Persani, L., and Lohse, M. J. (2009) Persistent cAMP-signals triggered by internalized G-protein-coupled receptors. *PLos Biol.* **7,** e1000172
8. Werthmann, R. C., Volpe, S., Lohse, M. J., and Calebiro, D. (2012) Persistent cAMP signaling by internalized TSH receptors occurs in thyroid but not in HEK293 cells. *FASEB J.* **26,** 2043–2048
9. Irannejad, R., and von Zastrow, M. (2014) GPCR signaling along the endocytic pathway. *Curr. Opin. Cell Biol.* **27,** 109–116
10. Lin, C. H., MacGurn, J. A., Chu, T., Stefan, C. J., and Emr, S. D. (2008) Arrestin-related ubiquitin-ligase adaptors regulate endocytosis and protein turnover at the cell surface. *Cell* **135,** 714–725
11. Aubry, L., and Klein, G. (2013) True arrestins and arrestin-fold proteins: a structure-based appraisal. *Prog. Mol. biol. Transl. Sci.* **118,** 21–56
12. Aubry, L., Guetta, D., and Klein, G. (2009) The arrestin fold: variations on a theme. *Curr. Genomics* **10,** 133–142
13. Gurevich, V. V., and Gurevich, E. V. (2006) The structural basis of arrestin-mediated regulation of G-protein-coupled receptors. *Pharmacol. Ther.* **110,** 465–502
14. Alvarez, C. E. (2008) On the origins of arrestin and rhodopsin. *BMC Evol. Biol.* **8,** 222
15. Nabhan, J. F., Pan, H., and Lu, Q. (2010) Arrestin domain-containing protein 3 recruits the NEDD4 E3 ligase to mediate ubiquitination of the β2-adrenergic receptor. *EMBO Rep.* **11,** 605–611
16. Rauch, S., and Martin-Serrano, J. (2011) Multiple interactions between the ESCRT machinery and arrestin-related proteins: implications for PPXY-dependent budding. *J. Virol.* **85,** 3546–3556
17. Puca, L., Chastagner, P., Meas-Yedid, V., Israël, A., and Brou, C. (2013) α-Arrestin 1 (ARRDC1) and β-arrestins cooperate to mediate Notch degradation in mammals. *J. Cell Sci.* **126,** 4457–4468
18. Qi, S., O'Hayre, M., Gutkind, J. S., and Hurley, J. H. (2014) Structural and

biochemical basis for ubiquitin ligase recruitment by arrestin-related domain-containing protein-3 (ARRDC3). *J. Biol. Chem.* **289,** 4743–4752
19. Han, S.-O., Kommaddi, R. P., and Shenoy, S. K. (2013) Distinct roles for β-arrestin2 and arrestin-domain-containing proteins in β2 adrenergic receptor trafficking. *EMBO Rep.* **14,** 164–171
20. Bache, K. G., Raiborg, C., Mehlum, A., and Stenmark, H. (2003) STAM and Hrs are subunits of a multivalent ubiquitin-binding complex on early endosomes. *J. Biol. Chem.* **278,** 12513–12521
21. Raiborg, C., Wesche, J., Malerød, L., and Stenmark, H. (2006) Flat clathrin coats on endosomes mediate degradative protein sorting by scaffolding Hrs in dynamic microdomains. *J. Cell Sci.* **119,** 2414–2424
22. Stenmark, H., Parton, R. G., Steele-Mortimer, O., Lütcke, A., Gruenberg, J., and Zerial, M. (1994) Inhibition of rab5 GTPase activity stimulates membrane fusion in endocytosis. *EMBO J.* **13,** 1287–1296
23. Hamdan, F. F., Percherancier, Y., Breton, B., and Bouvier, M. (2006) Monitoring protein-protein interactions in living cells by bioluminescence resonance energy transfer (BRET). *Curr. Protoc. Neurosci.* Chapter 5, Unit 5.23
24. Hislop, J. N., and von Zastrow, M. (2011) Analysis of GPCR localization and trafficking. *Methods Mol. Biol.* **746,** 425–440
25. Kang, D. S., Tian, X., and Benovic, J. L. (2013) β-Arrestins and G protein-coupled receptor trafficking. *Methods Enzymol.* **521,** 91–108
26. Temkin, P., Lauffer, B., Jäger, S., Cimermancic, P., Krogan, N. J., and von Zastrow, M. (2011) SNX27 mediates retromer tubule entry and endosome-to-plasma membrane trafficking of signalling receptors. *Nat. Cell Biol.* **13,** 715–721
27. Puthenveedu, M. A., Lauffer, B., Temkin, P., Vistein, R., Carlton, P., Thorn, K., Taunton, J., Weiner, O. D., Parton, R. G., and von Zastrow, M. (2010) Sequence-dependent sorting of recycling proteins by actin-stabilized endosomal microdomains. *Cell* **143,** 761–773
28. Hall, R. A., Premont, R. T., Chow, C. W., Blitzer, J. T., Pitcher, J. A., Claing, A., Stoffel, R. H., Barak, L. S., Shenolikar, S., Weinman, E. J., Grinstein, S., and Lefkowitz, R. J. (1998) The β2-adrenergic receptor interacts with the Na^+/H^+-exchanger regulatory factor to control Na^+/H^+ exchange. *Nature* **392,** 626–630
29. Cao, T. T., Deacon, H. W., Reczek, D., Bretscher, A., and von Zastrow, M. (1999) A kinase-regulated PDZ-domain interaction controls endocytic sorting of the β2-adrenergic receptor. *Nature* **401,** 286–290
30. Lauffer, B. E., Melero, C., Temkin, P., Lei, C., Hong, W., Kortemme, T., and von Zastrow, M. (2010) SNX27 mediates PDZ-directed sorting from endosomes to the plasma membrane. *J. Cell Biol.* **190,** 565–574
31. Steinberg, F., Gallon, M., Winfield, M., Thomas, E. C., Bell, A. J., Heesom, K. J., Tavaré, J. M., and Cullen, P. J. (2013) A global analysis of SNX27-retromer assembly and cargo specificity reveals a function in glucose and metal ion transport. *Nat. Cell Biol.* **15,** 461–471
32. Gallon, M., Clairfeuille, T., Steinberg, F., Mas, C., Ghai, R., Sessions, R. B., Teasdale, R. D., Collins, B. M., and Cullen, P. J. (2014) A unique PDZ domain and arrestin-like fold interaction reveals mechanistic details of endocytic recycling by SNX27-retromer. *Proc. Natl. Acad. Sci. U. S.* **111,** E3604–E3613
33. Irannejad, R., Kotowski, S. J., and von Zastrow, M. (2014) Investigating signaling consequences of GPCR trafficking in the endocytic pathway. *Methods Enzymol.* **535,** 403–418
34. Oka, S., Masutani, H., Liu, W., Horita, H., Wang, D., Kizaka-Kondoh, S., and Yodoi, J. (2006) Thioredoxin-binding protein-2-like inducible membrane protein is a novel vitamin D3 and peroxisome proliferator-activated receptor (PPAR)γ ligand target protein that regulates PPARγ signaling. *Endocrinology* **147,** 733–743
35. Dores, M. R., Lin, H., J Grimsey, N., Mendez, F., and Trejo, J. (2015) The α-arrestin ARRDC3 mediates ALIX ubiquitination and G protein-coupled receptor lysosomal sorting. *Mol. Biol. Cell* **26,** 4660–4673
36. Qi, S., O'Hayre, M., Gutkind, J. S., and Hurley, J. H. (2014) Insights into β2-adrenergic receptor binding from structures of the N-terminal lobe of ARRDC3. *Protein Sci.* **23,** 1708–1716
37. Patwari, P., Emilsson, V., Schadt, E. E., Chutkow, W. A., Lee, S., Marsili, A., Zhang, Y., Dobrin, R., Cohen, D. E., Larsen, P. R., Zavacki, A. M., Fong, L. G., Young, S. G., and Lee, R. T. (2011) The arrestin domain-containing 3 protein regulates body mass and energy expenditure. *Cell Metab.* **14,** 671–683
38. Shea, F. F., Rowell, J. L., Li, Y., Chang, T. H., and Alvarez, C. E. (2012) Mammalian α arrestins link activated seven transmembrane receptors to Nedd4 family E3 ubiquitin ligases and interact with β arrestins. *PLoS ONE* **7,** e50557
39. Shenoy, S. K., Xiao, K., Venkataramanan, V., Snyder, P. M., Freedman, N. J., and Weissman, A. M. (2008) Nedd4 mediates agonist-dependent ubiquitination, lysosomal targeting, and degradation of the β2-adrenergic receptor. *J. Biol. Chem.* **283,** 22166–22176
40. Shenoy, S. K., Modi, A. S., Shukla, A. K., Xiao, K., Berthouze, M., Ahn, S., Wilkinson, K. D., Miller, W. E., and Lefkowitz, R. J. (2009) β-Arrestin-dependent signaling and trafficking of 7-transmembrane receptors is reciprocally regulated by the deubiquitinase USP33 and the E3 ligase Mdm2. *Proc. Natl. Acad. Sci. U.S.A.* **106,** 6650–6655
41. Jean-Charles, P. Y., Rajiv, V., Shenoy, S. K. (2016) Ubiquitin-related roles of β-arrestins in endocytic trafficking and signal transduction. *J. Cell Physiol.*, 10.1002/jcp.25317
42. Tsvetanova, N. G., and von Zastrow, M. (2014) Spatial encoding of cyclic AMP signaling specificity by GPCR endocytosis. *Nat. Chem. Biol.* **10,** 1061–1065
43. Yao, X., Parnot, C., Deupi, X., Ratnala, V. R., Swaminath, G., Farrens, D., and Kobilka, B. (2006) Coupling ligand structure to specific conformational switches in the β2-adrenoceptor. *Nat. Chem. Biol.* **2,** 417–422
44. Rosenbaum, D. M., Cherezov, V., Hanson, M. A., Rasmussen, S. G., Thian, F. S., Kobilka, T. S., Choi, H.-J., Yao, X.-J., Weis, W. I., Stevens, R. C., and Kobilka, B. K. (2007) GPCR engineering yields high-resolution structural insights into β2-adrenergic receptor function. *Science* **318,** 1266–1273